IEEE Journal of Microwaves

Received 10 June 2021; revised 21 July 2021 and 14 August 2021; accepted 17 August 2021. Date of publication 23 September 2021; date of current version 7 October 2021.

Digital Object Identifier 10.1109/JMW.2021.3106871

Generalized One-Dimensional Parallel Switching Matrices With an Arbitrary Number of Beams

JIRO HIROKAWA [1] (Fellow, IEEE), AND NELSON J. G. FONSECA [2] (Senior Member, IEEE)

(Regular Paper)

[1]Department of Electrical and Electronic Engineering, Tokyo Institute of Technology, Tokyo 152-8552, Japan
[2]Antenna and Sub-Millimetre Waves Section, European Space Agency, NL-2200 AG Noordwijk, The Netherlands

CORRESPONDING AUTHOR: Jiro Hirokawa (e-mail: jiro@ee.e.titech.ac.jp).

ABSTRACT This paper introduces a novel family of one-dimensional switching matrices, also known as beamforming networks (BFNs), which can be sized for an arbitrary number of beams. It also describes the associated numerical design method, supported by several design examples. The concept is further validated with a full-wave model of a generic 5 × 5 switching matrix designed at 76 GHz. The proposed matrices are obtained by cascading units consisting of a two-way coupler and a phase shifter in a parallel configuration, providing theoretically lossless operation as a direct consequence of the orthogonal BFN topology and equalized path lengths, expected to benefit the frequency bandwidth. The design method is general, also including the configurations equivalent to Butler matrices when the number of beams is a power of two. The obtained planar matrix designs combine some benefits of the well-known Butler and Nolen matrices, namely the parallel topology and the arbitrary number of beams. The minimum number of cascaded units required by the proposed topology, also corresponding to the number of layers, is found to be N, where N is the number of beams, which is less than the number of cascaded units for the corresponding "parallel" Nolen matrix, for N larger than three, thus providing a reduction in the number of layers of up to 38% for an 8-beam matrix. This reduction is close to the theoretical upper boundary of 50%, reached for large values of N. This significant reduction is expected to have a positive impact on RF performance, and in particular insertion losses, as well as amplitude and phase dispersion over the operating band. Interestingly, the proposed switching matrix configuration reduces to a standard Butler matrix when the number of beams is equal to 4, and demonstrates a reduction in the number of layers of 20% over the corresponding planar Butler matrix for a design with 8 beams. The proposed matrix configuration is a promising solution for the design of low-cost single-layer beam-switching matrices.

INDEX TERMS Beamforming network (BFN), Butler matrix, millimeter-wave, multiple beam antenna, orthogonal beamformer, Nolen matrix, switching matrix.

I. INTRODUCTION

Multiple beam antennas are of interest for millimeter-wave applications, including next-generation terrestrial communication systems, collision avoidance systems, and small-space platform instruments. Beamforming networks (BFNs) generate multiple fixed beams from the same array antenna and are suitable for beam-switching microwave systems. They implement discrete beamforming techniques obtained with the interconnection of elementary components, such as power dividers, couplers and phase shifters. Well-known BFN solutions include Blass [1], Butler [2], and Nolen [3] matrices. Blass and Nolen matrices are characterized by a series-fed topology, while Butler matrices have a parallel-fed topology. The latter provides stable frequency operation thanks to equalized path lengths, while the former is naturally dispersive, introducing significant beam squint with frequency, even over

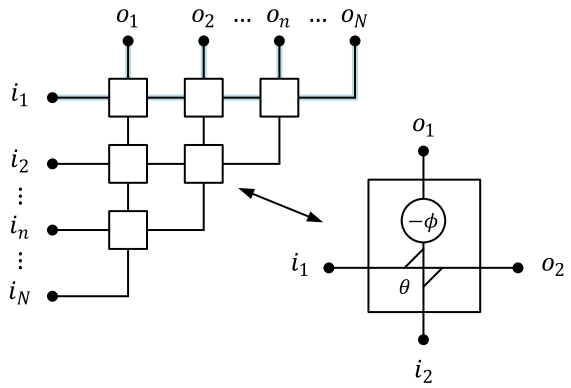

FIGURE 1. Standard Nolen matrix with series-fed topology (left) and constituting unit (right) [3], [23].

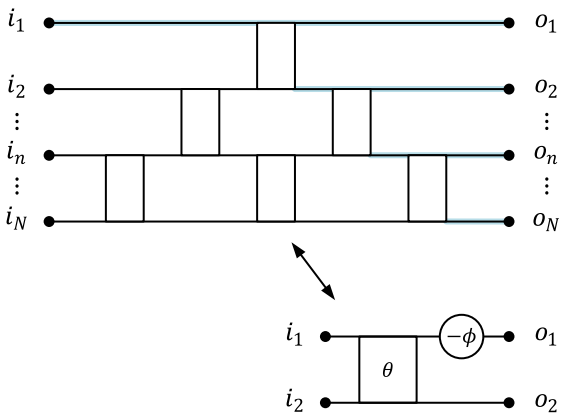

FIGURE 2. Parallel Nolen matrix with equalized path length (top) and constituting unit (bottom) [26].

narrow bandwidths [4]. The scattering matrices of Butler and Nolen matrices are unitary, indicating they are theoretically lossless [5]–[7]. Instead, Blass matrices are by definition lossy as they require the use of termination loads, which dissipate part of the signal. Of course, all matrices also have losses linked to the practical implementation, such as ohmic losses. Thus, a careful selection of the transmission line technology is important, particularly at millimeter-wave frequencies [8].

Over recent years, BFN theory and techniques have regained interest among researchers, mostly driven by 5G developments in the millimeter-wave range, as these solutions provide cost-effective alternatives to phased arrays when implemented in printed circuit board (PCB) technology [9]. In its standard form, the number of beams of a Butler matrix is limited to powers of two, while Blass and Nolen matrices are capable of generating an arbitrary number of beams. A generalized Butler matrix topology was proposed to produce a number of beams that is not a power of two [10]. However, the need for more complex building blocks (e.g. 3-way couplers) provides limited benefits over alternative solutions. As a consequence, this solution has attracted little interest from researchers, who have mostly reported 4 and 8 beam designs [11]–[22]. A number of works have also been reported on Nolen matrices in the past decade [23]–[29], as they preserve the theoretically lossless operation and orthogonal multiple beams of the Butler matrix, while introducing flexibility in the number of beams. In particular, the topology investigated in [26] is appealing as it equalizes the path lengths through a "parallel" arrangement, resulting in a broad frequency band operation similar to that of a Butler matrix.

Standard Nolen matrices are composed of cascading units or nodes with a series-fed topology characterised with vertical array element transmission lines and horizontal feeding port transmission lines, schematically shown in Fig. 1. The unit, illustrated as an inset in Fig. 1, consists of a two-way coupler and a phase shifter, enabling any amplitude imbalance and phase difference between the two output ports of each unit. It also corresponds to the elementary matrix with 2 beams. The configuration of standard Nolen matrices for any number of beams can be defined straightforwardly, thanks to their simple series-fed topology, and a numerical design method is available [23]. The general form of the Nolen matrix enables to have a number of inputs, M, that differs from the number of outputs, N. However, theoretically lossless operation in both transmit and receive requires $M = N$ [7], which is the configuration considered in this paper. Furthermore, the number of cascaded units from a given input port to any given output port varies. This is evidenced in Fig. 1 highlighting the paths connecting the input port i_1 to each output port o_n, for $n = 1...N$, where the number of cascaded units varies from 1 to $N - 1$. Thus, coupler delay compensation together with path length equalisation was proposed to achieve broadband performance [26]. This alternative topology, referred to as a "parallel" Nolen matrix configuration, is schematically illustrated in Fig. 2 with its associated unit cell as an inset. The unit is actually the same as in the standard case, only the arrangement of the ports is different to adapt to the new topology. The paths connecting the input port i_1 to all output ports o_n, for $n = 1...N$, are also highlighted in Fig. 2 to emphasise the benefits of the parallel arrangement. By analogy with the fast Fourier transform [30], [31], Butler matrices are the parallel-fed topology assumed to require the least number of units. However, this leads to transmission line crossovers, with their number increasing drastically with the number of beams, making them less attractive for single-layer PCB implementation.

In this paper, a modified Nolen matrix topology is proposed. A general configuration cascading the units for any number of beams is introduced, adapted from the concept of chess networks [32], [33], used in the design of overlapping sub-arrays with reduced field of view. The proposed configuration provides a more balanced distribution of components per input ports when compared to the "parallel" Nolen matrix. It is found that the proposed generalized switching matrix reduces to a Butler matrix when the number of beams is equal to 4, and is more compact in the case of an 8-beam matrix design. Also, the minimum number of cascaded units from the input port side to the output port side is provided as a function of the number of beams, up to 8 beams, and is found to be smaller than that

of the Nolen matrix when the number of beams is larger than three, resulting in a reduction in the number of layers for the analyzed matrices of up to 38% in a single-layer implementation. Further reduction is achieved as the number of beams increases, making the proposed configuration particularly suitable for planar designs requiring a larger number of beams. The paper is organized as follows. Section II introduces the proposed generalized parallel matrix and its design method. Design examples are detailed in Section III, including a specific implementation of a 5×5 parallel matrix designed at 76 GHz to validate the presented theory, as well as a general matrix topology description with an even number of beams. A detailed comparison with reference Nolen and Butler matrices is also provided. Finally, some conclusions and perspective of future works are gathered in Section IV.

II. GENERALIZED PARALLEL MATRIX CONFIGURATION

A. DESCRIPTION

The proposed matrix uses the same one-dimensional unit consisting of a one-plane coupler and a phase shifter, as also used in the standard and parallel Nolen matrices of Fig. 1 and Fig. 2. The phase shifter is connected to the output port o_1 for the purpose of this development. Equivalent results would be obtained with a phase shifter connected to the output port o_2, as only relative phase matters. Throughout this paper, the following convention is used: when feeding from port i_1, i_2 is referred to as the isolated port, o_1 as the direct port and o_2 as the coupled port.

The unit is characterized by its scattering matrix $\mathbf{S}$. It is assumed to have all ports perfectly matched, and the two input ports, respectively the two output ports, mutually decoupled. Assuming that all power applied at one input port is fully distributed to the two output ports, corresponding to the theoretically lossless operation discussed in the introduction, requires the matrix $\mathbf{S}$ to be unitary. This can be written as $\mathbf{S}^T \cdot \mathbf{S}^* = \mathbf{I}$, where $\mathbf{S}^T$ and $\mathbf{S}^*$ are the transpose and complex conjugate of $\mathbf{S}$, respectively, and $\mathbf{I}$ is the identity matrix. The unit is thus fully characterized by the reduced matrix containing the transmission coefficients, referred to as the transmission matrix $\mathbf{T}$, such that:

$$\begin{bmatrix} o_1 \\ o_2 \end{bmatrix} = \mathbf{T} \begin{bmatrix} i_1 \\ i_2 \end{bmatrix} \tag{1}$$

The matrix $\mathbf{T}$ is defined in a parametric form as follows

$$\mathbf{T} = \begin{bmatrix} \cos\theta e^{-j\phi} & -j\sin\theta e^{-j\phi} \\ -j\sin\theta & \cos\theta \end{bmatrix} \tag{2}$$

where θ is the coupling factor and ϕ is the delay introduced by the phase shifter. When $\theta = 0$, the coupler sends all the power to the direct port and reduces to two unconnected transmission lines. When $\theta = \pi/2$, the coupler becomes a crossover junction, meaning that all the input power is transmitted to the coupled port. The value of θ is restricted to the interval $[0, \pi/2]$ without loss of generality, as any value of θ may be reduced to that interval with an adequate phase correction of π either on the input or on the output ports to account for negative values of $\cos\theta$, of $\sin\theta$, or of both simultaneously. The two-way coupler is assumed to be a quadrature coupler, meaning that the coupled port has a phase delay of $\pi/2$ with respect to the direct port on top of the phase delay introduced by the phase shifter.

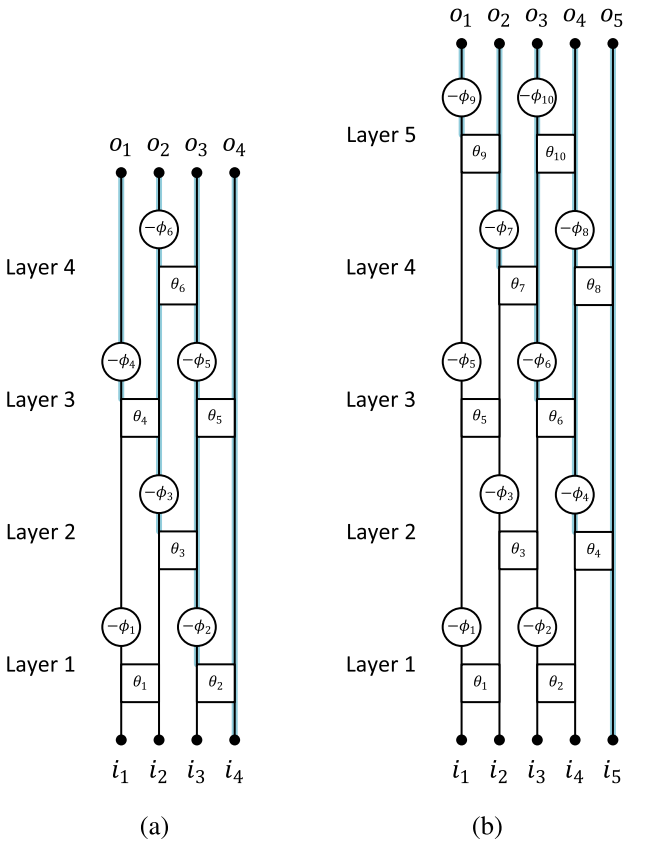

FIGURE 3. Proposed generalized one-dimensional parallel switching matrix (a) with four beams and (b) with five beams.

The general configuration of the proposed parallel matrix is different for even and odd numbers of beams. Fig. 3(a) shows the general configuration of the matrix with four beams, or 4×4 matrix, as an example of even numbers of beams, while Fig. 3(b) shows that with five beams, or 5×5 matrix, as an example of odd numbers of beams. For an even number N of beams, $N/2$ units are arrayed in an odd layer, and $(N-2)/2$ units are arrayed in an even layer. The units in the odd layers and those in the even layers are shifted by one port. For an odd number N of beams, $(N-1)/2$ units are arrayed both in odd and even layers. The units in the odd layers and those in the even layers are also shifted by one port.

Comparing the matrix configuration in Fig. 2 for $N = 4$ with the proposed matrix in Fig. 3(a), it is apparent that the proposed geometry can achieve some reduction in the number of layers. Indeed, comparing the paths highlighted in both schematics, it appears that a minimum of 5 layers is required in Fig. 2 to distribute the signal from any input port to all output ports. The limiting input port is the first one, i_1. With the proposed matrix, the parallel topology enables to distribute

the signal from any input port to all output ports after only 3 layers. More generally, for an even number of beams, the proposed topology would require at least $N-1$ layers to distribute the power from any input port towards all output ports, this minimum value being imposed by the diagonal path, i.e. the path connecting the input port i_N to the output port o_1, highlighted in Fig. 3(a), but also the path connecting the input port i_1 to o_N, due to the symmetry in the topology. This constrains the minimum achievable number of layers for a given value of N, when N is even. A topology with less layers would result in an overlapping sub-array design, where each input port would feed only a subset of output ports [32], [33]. For odd number of beams, the asymmetry of the topology, evidenced in Fig. 3(b), requires an additional layer to distribute the power from the last input port towards all output ports, the constraint coming here also from the diagonal path connecting the input port i_N to o_1. The corresponding path is highlighted in Fig. 3(b). Thus, from a topological point of view, the number of layers cannot be smaller than $N-1$ for an even number of beams and N for an odd number of beams. In practice, no solution has been found with $N-1$ layers when N is an even number. This is the reason the matrix with 4 beams in Fig. 3(a) is illustrated with 4 layers.

B. DESIGN METHOD

Following the layer matrix approach also used in [34], we introduce the transmission matrix $\mathbf{T}_l$, where l is the index of the layer, which varies from 1 to L, L being the total number of layers, such that

$$\mathbf{a}_{l+1} = \mathbf{T}_l \cdot \mathbf{a}_l \tag{3}$$

where $\mathbf{a}_l$ and $\mathbf{a}_{l+1}$ are the input and output vectors of the considered layer, respectively. The transmission matrix $\mathbf{T}_{N\times N}$ of a matrix with N beams, such that $\mathbf{o} = \mathbf{T}_{N\times N} \cdot \mathbf{i}$, where $\mathbf{i}$ and $\mathbf{o}$ are the input and output vectors of the matrix, respectively, can thus be written

$$\mathbf{T}_{N\times N} = \prod_{l=1}^{L} \mathbf{T}_l \tag{4}$$

With the general description discussed in Section II.A and Fig. 3, the definition of the layer matrices $\mathbf{T}_l$, for $l = 1\ldots L$, as a function of unit parameters is straightforward and may be defined in a generic way, distinguishing between odd and even layers. These are reported in Appendix. This matrix formulation provides a numerical representation of the proposed parallel matrices.

The lossless condition constrains the transmission matrix, which can be uniquely written as [6]

$$\mathbf{T}_{N\times N} = \frac{1}{\sqrt{N}} \begin{bmatrix} 1 & 1 & \ldots & 1 \\ \rho_1 & \rho_2 & \ldots & \rho_N \\ \vdots & \vdots & \ddots & \vdots \\ \rho_1^{N-1} & \rho_2^{N-1} & \ldots & \rho_N^{N-1} \end{bmatrix}_{N\times N} \tag{5}$$

where ρ_n, for $n = 1\ldots N$, are the N distinct roots of unity. Note that this formulation is based on relative phase values per input port, and does not necessarily correspond to the absolute phases of an actual matrix implementation. These parameters may be conveniently written as

$$\rho_n = e^{+jp_n}, \quad \text{for } n = 1\ldots N \tag{6}$$

where p_n, for $n = 1\ldots N$, are the phase gradients for each input port i_n. For an orthogonal matrix with dimension $N \times N$, corresponding to a matrix with N beams, the phase difference p_k, for $k = 1\ldots N$, takes the following values in a range from $-\pi$ to $+\pi$ in the wave-number visible region [35]

$$p_k = \frac{2k\pi}{N} - \frac{(N+1)\pi}{N}, \quad \text{for } k = 1\ldots N \tag{7}$$

Each value of p_n, for $n = 1\ldots N$, should uniquely correspond to one value of p_k, for $k = 1\ldots N$, defining a bijection between the two sets of values carefully selected so that the unit parameters θ and ϕ of the complete matrix may be determined. Note that there is not a unique correspondence between the two sets of values. However, this correspondence may have an impact on the minimum achievable number of layers. Owing to the generic form of the proposed matrices, a number of permutations were found to achieve the minimum number of layers reported. In fact, all possible permutations were found to provide a numerical solution in the case of a matrix with N beams and N layers for N ranging between 3 and 6. Further investigations are required to confirm this remains valid for any value of N. Table I lists the specific values of phase differences p_n, for $n = 1\ldots N$, with assignment patterns, for $N = 2\ldots 8$, for which the values of θ and ϕ in this paper have been determined. The assignment method described by Moody for Butler matrices [35] only works when N is a power of two. Nevertheless, some of the design rules were found beneficial for the general configuration proposed here. The first one is to take advantage of the symmetry and assign phase differences with opposite signs to symmetric ports. This is valid when N is even and applied by extension also when N is odd, excluding the phase difference equal to zero. The second design rule is to set pairs of phase differences corresponding to the input ports of a same coupler of the first layer such that the sum of their absolute values is equal to π when N is even. This leads to a first layer with hybrid couplers only, having a coupling factor θ with a value of 0.25π. This is extended also to matrix designs with odd values of N by pairing phase differences such that the sum is $(N+1)\pi/N$. Finally, the signs of the phase differences are set to alternate as the index of the input port increases, starting with the lowest positive and non-zero phase difference.

The unknown values of θ and ϕ in all the units are determined numerically by solving a set of non-linear equations [33]. For the analyzed matrices, the minimum number of layers achieved with the proposed method is N for all values of N, independently if N is odd or even, excluding the elementary case $N = 2$. Both the number of unknowns and the number of non-linear equations are equal to $N(N-1)$, when

TABLE 1. Values of p_n for $n = 1...N$ and $N = 2...8$

$N=2$	$N=4$	$N=6$	$N=8$
			$p_1 = \frac{\pi}{8}$
		$p_1 = \frac{\pi}{6}$	$p_2 = \frac{-7\pi}{8}$
	$p_1 = \frac{\pi}{4}$	$p_2 = \frac{-5\pi}{6}$	$p_3 = \frac{5\pi}{8}$
$p_1 = \frac{\pi}{2}$	$p_2 = \frac{-3\pi}{4}$	$p_3 = \frac{3\pi}{6}$	$p_4 = \frac{-3\pi}{8}$
$p_2 = \frac{-\pi}{2}$	$p_3 = \frac{3\pi}{4}$	$p_4 = \frac{-3\pi}{6}$	$p_5 = \frac{3\pi}{8}$
	$p_4 = \frac{-\pi}{4}$	$p_5 = \frac{5\pi}{6}$	$p_6 = \frac{-5\pi}{8}$
		$p_6 = \frac{-\pi}{6}$	$p_7 = \frac{7\pi}{8}$
			$p_8 = \frac{-\pi}{8}$

$N=3$	$N=5$	$N=7$
		$p_1 = \frac{2\pi}{7}$
	$p_1 = \frac{2\pi}{5}$	$p_2 = \frac{-6\pi}{7}$
$p_1 = \frac{2\pi}{3}$	$p_2 = \frac{-4\pi}{5}$	$p_3 = \frac{4\pi}{7}$
$p_2 = \frac{-2\pi}{3}$	$p_3 = \frac{4\pi}{5}$	$p_4 = \frac{-4\pi}{7}$
$p_3 = 0$	$p_4 = \frac{-2\pi}{5}$	$p_5 = \frac{6\pi}{7}$
	$p_5 = 0$	$p_6 = \frac{-2\pi}{7}$
		$p_7 = 0$

the number of layers is equal to N, thus the problem can be solved and has a unique solution for a given permutation of the phase gradients p_n, for $n = 1...N$, when θ is restricted to the interval $[0, \pi/2]$. The number of unknowns is a consequence of the topology of the matrices, while the number of equations is obtained with the condition on the phase differences between adjacent output ports for all input ports. As a curiosity, the proposed matrix and the corresponding Nolen matrix have the same number of units, also independently if N is odd or even. Thus, the proposed solution does not increase the complexity of the design, but instead, arranges differently the same number of units to achieve a more compact configuration with less layers. Section III provides numerical examples of the proposed beam-switching matrix solution which support the description of a general topology for the proposed matrices.

TABLE 2. Values of θ/π and ϕ/π in the Matrix With Four Beams

Unit	θ/π	ϕ/π
1	0.250	0.750
2	0.250	0.250
3	0.500	0.000
4	0.250	-0.500
5	0.250	0.500
6	0.500	0.000

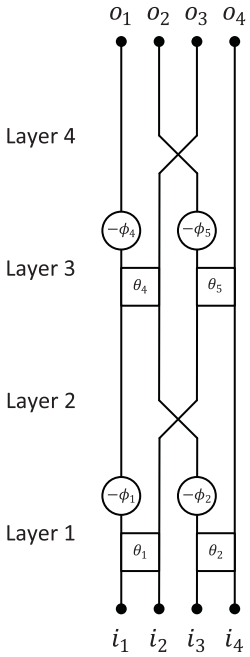

FIGURE 4. Simplified parallel matrix with four beams, including crossover junctions and merged phase shifters.

III. NUMERICAL RESULTS

A. PARALLEL MATRIX WITH FOUR BEAMS

The minimum number of layers in the matrix with four beams achieved with the proposed method is four. With that configuration, the values of θ and ϕ in all the units, as shown in Fig. 3(a), can be determined. The number of the unknown values, θ and ϕ, and the number of non-linear equations are both equal to 12. Table II lists the values of θ/π and ϕ/π for the corresponding set of p_n, for $n = 1...4$, given in Table I.

It is noted that Units 3 and 6 become crossover junctions. The corresponding phase shifters only affect one path and can thus be combined with the phase shifters of the units before the respective crossovers and connected to input ports i_2, with the Unit notations provided in Fig. 2. For this specific design, phase shifters 2 and 3 in Fig. 3(a) can be combined into one phase shifter. Phase shifters 5 and 6 in Fig. 3(a) can be combined as well. The values in Table II account for this merge, and the phase shits of the crossovers are set to zero. Fig. 4 shows the configuration including the crossover junctions and merged phase shifters. Interestingly, this configuration is equivalent to that of the well-known Butler

TABLE 3. Values of θ/π and ϕ/π in the Matrix With Five Beams

Unit	θ/π	ϕ/π
1	0.250	0.800
2	0.176	-0.200
3	0.387	0.524
4	0.276	0.431
5	0.272	-0.524
6	0.346	-0.331
7	0.387	0.200
8	0.276	-0.700
9	0.250	-0.500
10	0.324	-0.700

matrix obtained by the conventional method relating to the fast Fourier transform [2], [10], [35]. However, the positions of the phase shifters and the values of the phase shifts are different because of the generic Unit configuration. The phase shifter 2, introducing a phase delay of $-\phi_2$ at the direct output port in Unit 2, can be replaced with a phase shifter having a phase delay of $+\phi_2$ placed at the coupled output port. Another consequence of the selected Unit and associated generic transmission matrix is that a crossover junction introduces a phase delay of $\phi = \pi/2$. In particular, the phase delays in Units 4 and 5 are solely compensating for the crossover junction phase delay. Thus, with these phase shift equivalences, the proposed matrix reduces to a standard Butler matrix in this specific case. In a practical realization, differences among transmission lines and couplers or crossovers in terms of transmission phase should be compensated in each layer, similarly to what was implemented in [26]. Adjusting the topology by modifying some Units may also bring some size reduction in practical implementations. For instance, the phase shifters ϕ_2 and ϕ_5 in Layer 3, as per notations in Fig. 4, may be implemented in parallel of the crossover junction in Layer 4, thus leading to a more compact implementation, similar to that of the 4×4 Butler matrix described in [18].

B. PARALLEL MATRIX WITH FIVE BEAMS

The minimum achieved number of layers in the matrix with five beams is five. The corresponding topology is shown in Fig. 3(b). The number of the unknown values of θ and ϕ is 20, and the number of the non-linear equations is also 20. Table III lists the values of θ/π and ϕ/π for the corresponding set of p_n, for $n = 1\ldots5$, given in Table I. In this case, there are no simplifications identified and the resulting matrix has the generic topology illustrated in Fig. 3(b).

This numerical solution is not unique as different matrix configurations were found to achieve the same minimum number of layers when permuting the phase gradients p_n, for $n = 1\ldots N$. In fact, there is a total of $N!$ permutations, thus 120 possible cases when $N = 5$, as the reduction in permutations with the considerations derived from the work of Moody [35] are not really applicable when N is odd. Further investigations would be required to find the optimum configuration leading to the most compact and less dispersive matrix design. Due to its generic configuration, this is however a good test case to validate the presented method with a specific matrix design and implementation in substrate integrated waveguide (SIW) technology [8]. The only modification brought to the numerical example in Table III is the phase shift value in Unit 1, which is changed to -0.2π, resulting in a smaller value and thus shorter phase shifter design. This is achieved by simply swapping the phase gradients, p_1 and p_2, of ports 1 and 2. All remaining Units are kept unchanged.

The complete full-wave model of the 5×5 parallel matrix was developed using the frequency domain FEM solver of Ansys HFSS. For a better comparison with the 4×4 parallel Nolen matrix described in [26], similar assumptions are considered here. The design frequency is 76 GHz and the substrate material has the characteristics of the Rogers RT/duroid 6002 laminate, with a relative permittivity of 2.94, tangent losses of 0.0012 and a thickness of 0.508 mm. For the purposes of this validation, a design based on an equivalent rectangular waveguide model is sufficient, with a broad wall dimension $a = 1.7$ mm [8]. A Riblet coupler is used, with the narrow wall waveguide aperture being adjusted to achieve the desired coupling value. The phase shifters are implemented varying the broad wall waveguide dimension of the transmission lines connecting the couplers. This is suitable for a compact implementation, in line with the constraints of the parallel design. However, this is more dispersive than the unequal length phase shifters used in [26] to achieve coupler delay compensation, indicating that the reported performance may be further improved. The key design parameters of a Unit using these two components are defined in Fig. 5(a). Note that the phase shifter may be implemented at the direct port or at the coupled port or at both ports simultaneously, taking advantage of the fact that only relative phases are important in a BFN design to achieve the most compact and less dispersive design. The phase shift may also be distributed across adjacent layers when convenient for further integration, particularly for the Units on the edge of the structure, reducing also the length of the structure. A single step Riblet coupler is considered here to simplify the design and reduce the number of parameters. A multiple step design may be implemented to further enhance the performance of the matrix [26]. A single step is sufficient for validation purposes. The final matrix design is illustrated in Fig. 5(b) and the optimized values of the design parameters are reported in Table IV. To maintain the parallel and straight transmission lines design, some Units had to be adapted to accommodate the phase shifter of the adjacent Unit. This is the case for Unit 6 and Unit 8, adapting to Unit 5 and Unit 7, respectively. When large phase shift values were required, the phase shift was split between the two output ports, with an increase of the broad wall dimension on one side and a complementary decrease on the other, as illustrated in Fig. 5(a), to reduce the overall length of the phase shifting section. This was implemented in Unit 3 and Unit 4. Interestingly, the functional area of this 5×5 parallel matrix design is 6 cm $\times$ 1 cm, which is the same as that of the

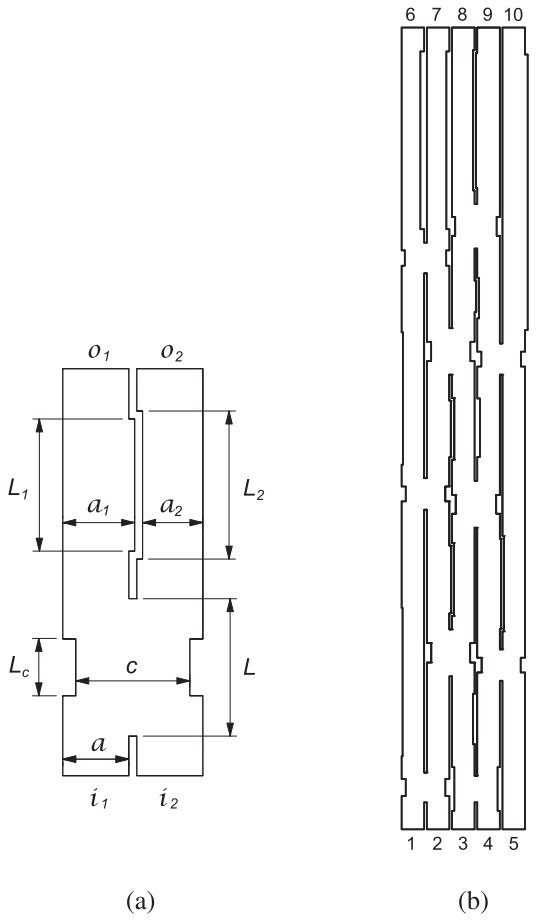

FIGURE 5. 5 × 5 parallel switching matrix at 76 GHz: (a) design parameters of a Unit and (b) complete matrix.

TABLE 4. Values of the Design Parameters in the 5 × 5 Parallel Switching Matrix at 76 GHz (in Wavelengths)

Unit	L	L_c	c	L_1	a_1	L_2	a_2
1	0.66	0.38	0.88	3.30	0.48	-	-
2	0.59	0.97	0.96	1.12	0.46	-	-
3	1.04	0.43	0.86	1.50	0.54	1.62	0.46
4	0.70	0.33	0.87	2.00	0.53	2.12	0.47
5	0.70	0.33	0.88	2.94	0.47	1.25	0.53
6	1.04	0.42	0.90	1.37	0.45	1.30	0.44
7	1.03	0.43	0.87	-	-	0.70	0.54
8	0.69	0.33	0.88	0.90	0.46	6.12	0.56
9	0.68	0.34	0.92	3.95	0.42	3.95	0.43
10	0.99	0.42	0.92	3.12	0.47	3.00	0.53

4 × 4 Nolen matrix with coupler delay compensation reported in [26]. With dimensions normalized to the wavelength in the dielectric material, the matrix has an area of $26.1\times4.3\lambda^2$. For comparison, the standard 4×4 Nolen matrix in [24] has a normalized area of $8.7\times6.7\lambda^2$, corresponding to a smaller area by a factor of 2 when compared to the parallel configuration. As anticipated, the standard design is more compact but has significantly reduced operating bandwidth as evidenced here.

The numerical results of the final matrix design over the frequency bandwidth $70-82$ GHz, corresponding to a fractional bandwidth of 15.8% centered at 76 GHz, are reported in Fig. 6. The numerical results in amplitude are reported from input port 1 to input port 5 in Fig. 6(a) to Fig. 6(e), respectively. The Units were optimized separately for a reflection coefficient and port-to-port isolation better than -20 dB, while these parameters remain mostly below -15 dB for the complete BFN, showing a stable and broadband response. The transmission coefficients are also quite stable over frequency, with a mean value of -7.98 dB at the design frequency, compared to a theoretical value of -6.99 dB. The difference is due to insertion losses, which are slightly higher than the 0.7 dB reported in [26] because of the simpler structure with slightly higher reflections. The design at Ku-band of a standard 4 × 4 Nolen matrix in [24] has average insertion losses of 0.75 dB. However, they report a strong variation per input port, with the worst case being up to 1.2 dB, while the parallel design described in this section provides very similar insertion losses for all ports. Compared to the parallel design in [26], transmission coefficients show a slightly higher amplitude dispersion, with a variation below ±0.5 dB over the frequency bandwidth $75.1-77.9$ GHz, corresponding to a fractional frequency bandwidth of 3.7%. This amplitude dispersion is equivalent to that reported for the standard Nolen matrix in [24], which uses the same type of phase shifters. The fractional frequency bandwidth may be extended to 11.9% over the range $72.1-81.2$ GHz considering an amplitude variation better than ±1 dB. These variations are mostly the consequence of the dispersive phase shifters, which affect amplitude variation when signals are recombined with a phase error translating into an amplitude error. These results may be improved introducing phase shifters with wider bandwidth characteristics.

The phase differences between adjacent ports are gathered for all input ports in Fig. 6(f). Average phase differences at 76 GHz are -143.6°, 73.7°, 145.0°, -70.0° and 0.1° for input ports 1 to 5, compared to -144°, 72°, 144°, -72° and 0° in theory. The average phase dispersion is better than $\pm12^\circ$ within the frequency range $72.4-82.0$ GHz, similar to the simulated performance reported in [26]. The design presented here shows stronger variations in the lower frequency range, up to $\pm30^\circ$ for port 3 at 70 GHz. This is mostly due to the phase shifter design, which is more dispersive closer to cut-off frequency. The designed matrix has a residual frequency-dependence on the average phase difference, with a visible positive slop in Fig. 6(f). This frequency-dependence is not present in the 4 × 4 Nolen matrix with coupler delay compensation [26], but is present in the standard Nolen matrix [24]. For comparison, a phase difference variation over frequency of $\pm20^\circ$ occurs over the frequency range $12.25-12.75$ GHz, corresponding to a fractional bandwidth of 4%. With the parallel design presented here, a similar variation is observed over the frequency band $71.1-82$ GHz, corresponding to a fractional bandwidth of at least 14.2%, as the variation is still within the limits at the upper frequency bound. This result

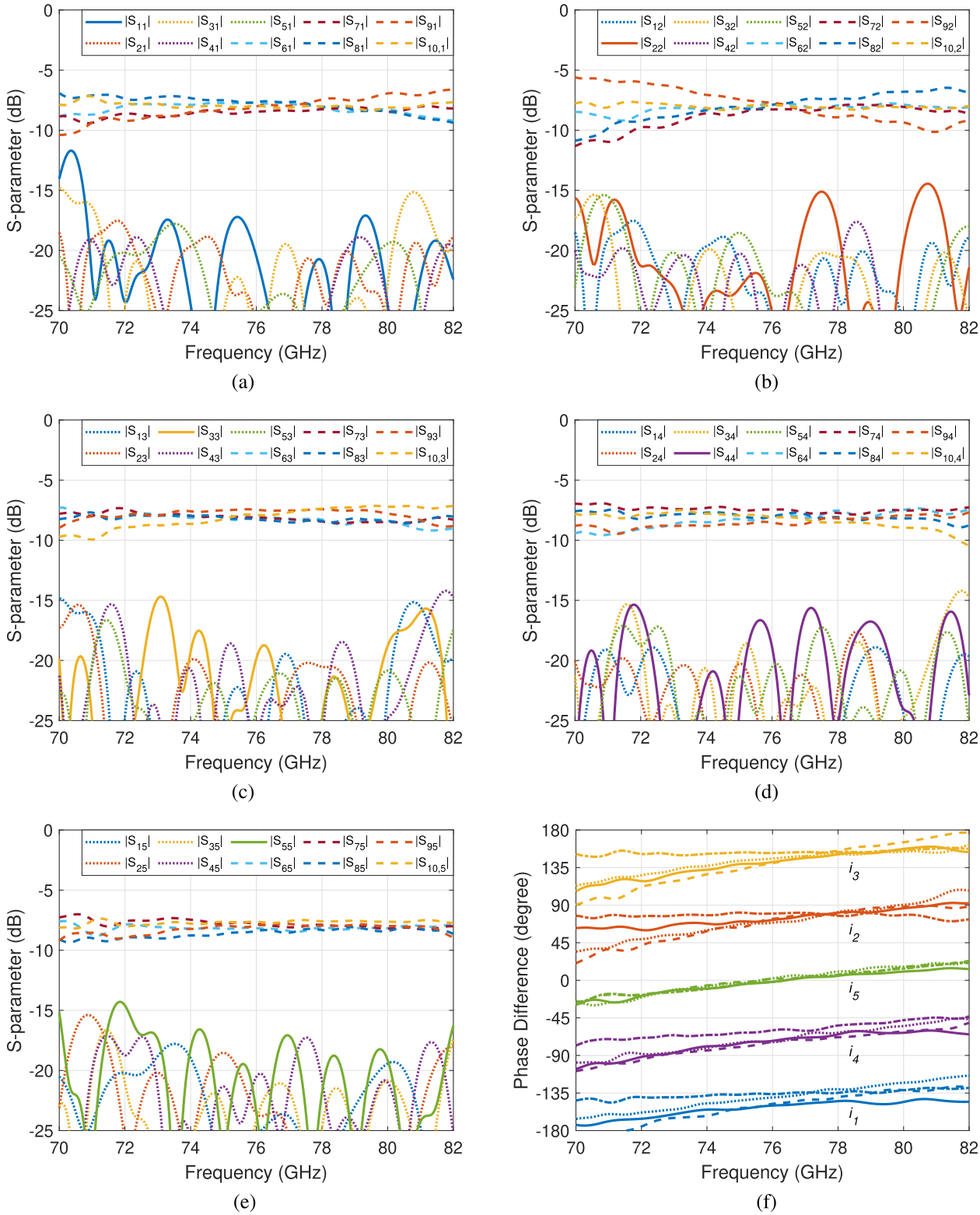

FIGURE 6. S-parameters of the 5 × 5 parallel switching matrix full-wave model: (a)-(e) amplitude in dB (reflection coefficients in *solid line*, port-to-port isolations in *dotted lines* and transmission coefficients in *dashed line*) and (f) phase difference between adjacent ports in degree (between port 7 and port 6 in *solid lines*, between port 8 and port 7 in *dashed lines*, between port 9 and port 8 in *dotted lines* and between port 10 and port 9 in *dashed-dotted lines*).

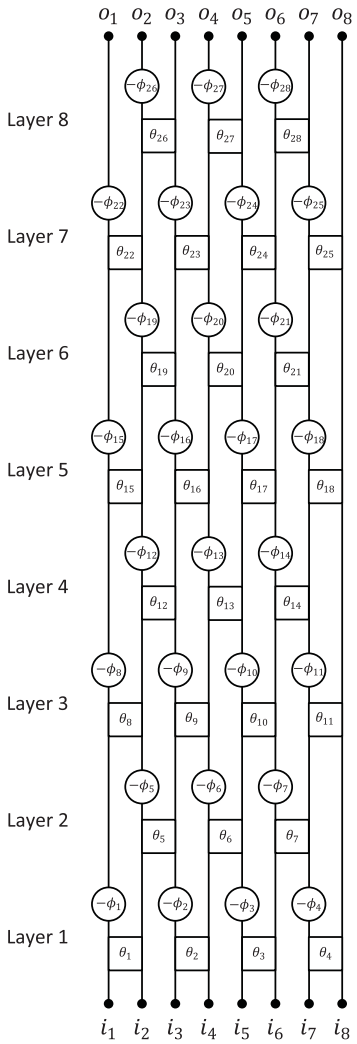

FIGURE 7. General configuration of the proposed parallel matrix with eight beams.

clearly demonstrates the benefits of the proposed parallel design, which may be further improved introducing the coupler delay compensation described in [26]. Overall, the achieved results are promising despite the simplifications considered. A refined design of the couplers and phase shifters is expected to also further enhance the response of the matrix or reduce its dimensions.

C. PARALLEL MATRIX WITH EIGHT BEAMS

The minimum number of layers in the matrix with eight beams is 8, as shown in Fig. 7. The number of the unknown values of θ and ϕ is 56, and the number of the non-linear equations is also 56. Table V lists the values of θ/π and ϕ/π for the corresponding set of p_n, for $n = 1..8$, given in Table I.

Units 5, 6, 7, 9, 10, 13, 20, 23, 24, 26, 27 and 28 take the value $\theta = 0.5\pi$, so they become crossover junctions. As in Section III.A, phase shifters before and after a crossover junction can be merged, as the amount of phase shift can be summed. Fig. 8 shows the resulting configuration including the crossover junctions and merged phase shifters. Interestingly, this particular matrix topology shows a distribution of crossovers which differs from that of the standard Butler matrix. A schematic representation of a standard 8×8 Butler matrix is also provided in Fig. 8 for comparison. The proposed matrix has 16 regular couplers and 12 crossover junctions, while the standard Butler matrix has 12 hybrid couplers and 16 crossover junctions. This particular arrangement is also found in the matrix with 6 beams using the corresponding set of p_n, for $n = 1...6$, given in Table I and may be extended to

TABLE 5. Values of θ/π and ϕ/π in the Matrix With Eight Beams

Unit	θ/π	ϕ/π
1	0.250	0.625
2	0.250	0.125
3	0.250	0.875
4	0.250	0.375
5	0.500	0.000
6	0.500	0.000
7	0.500	0.000
8	0.250	-0.750
9	0.500	0.000
10	0.500	0.000
11	0.250	-0.500
12	0.304	0.750
13	0.500	0.000
14	0.304	0.000
15	0.333	0.750
16	0.333	-0.250
17	0.333	0.750
18	0.333	1.000
19	0.304	-0.250
20	0.500	0.000
21	0.304	0.500
22	0.250	-0.250
23	0.500	0.000
24	0.500	0.000
25	0.250	0.250
26	0.500	0.000
27	0.500	0.000
28	0.500	0.000

TABLE 6. Minimum Number of Layers in Various Beam-Switching Matrices and Reduction Achieved With the General Solution

Number of beams	General matrix	Nolen matrix (Butler matrix)	Reduction (%)
2	1	1	0
3	3	3	0
4	4	5 (4)	20 (0)
5	5	7	29
6	6	9	33
7	7	11	36
8	8	13 (10)	38 (20)

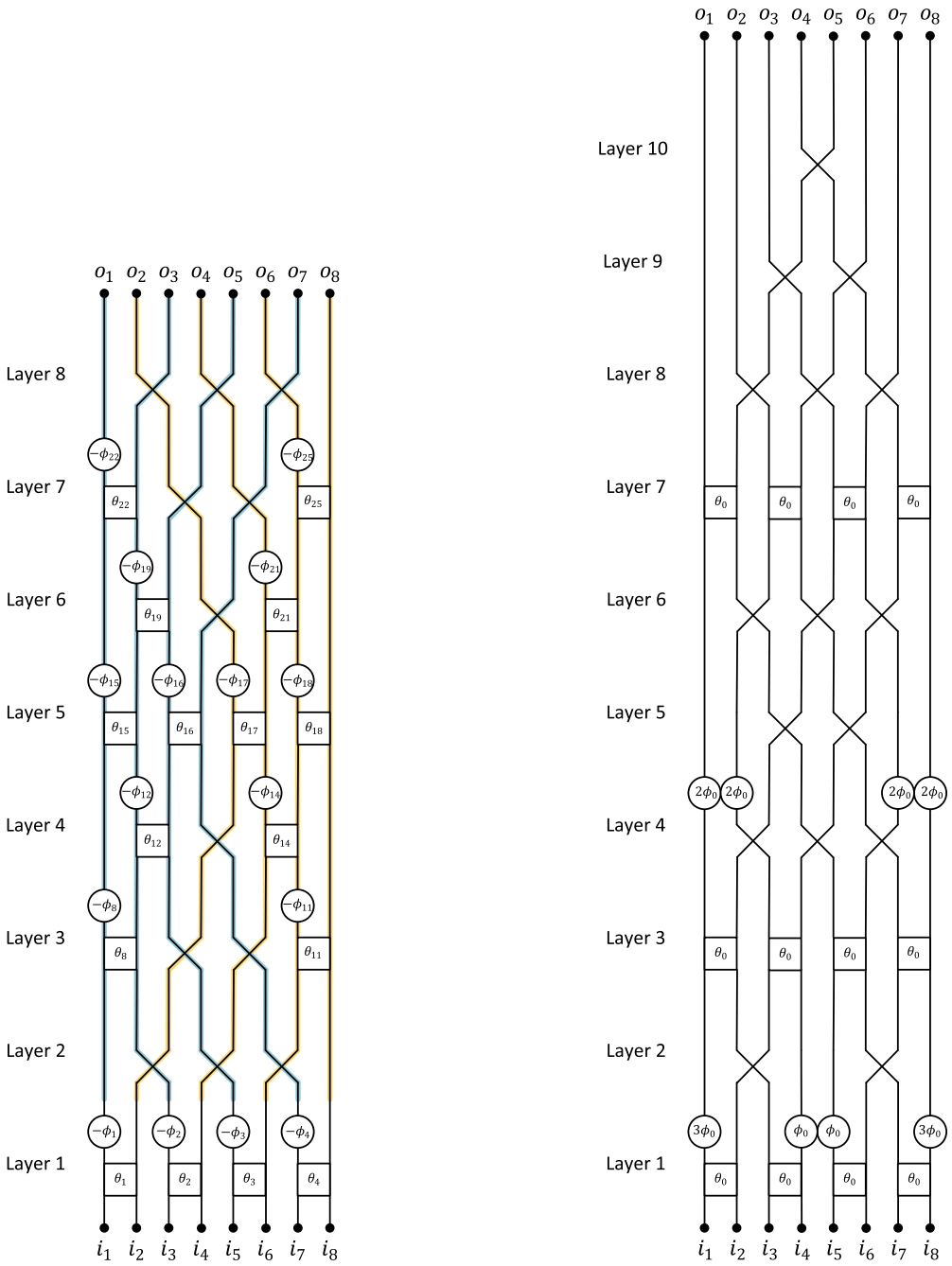

FIGURE 8. Simplified matrix with eight beams (left), including crossover junctions and merged phase shifters, compared to a standard 8x8 Butler matrix (right), with parameters $\theta_0 = \pi/4$ and $\phi_0 = -\pi/8$ (the assignment of phase gradients p_n, for $n = 1...N$, is the same for both matrices).

larger Butler matrices. This general topology is discussed in Section III.D.

D. GENERAL PARALLEL MATRIX CONFIGURATION WITH AN EVEN NUMBER OF BEAMS

While a general matrix configuration is not straightforward for an odd number of beams, an interesting topology can be identified when N is even. This derives from the observation that the 8×8 matrix in Fig. 8 is the combination of two parallel Nolen matrices of size 4×4, connected through a first layer of hybrid couplers with some obvious symmetries in the phase shifters due to the symmetry in the phase differences assignment. The Nolen matrix on the left side is constituted of the Units 8, 12, 15, 16, 19 and 22, while the Nolen matrix on the right side is constituted of the Units 11, 14, 17, 18, 21 and 25. The interconnection between the two parallel Nolen matrices and interleaved output ports lead to the arrangement of crossover junctions observed in Fig. 8, where the two matrices are highlighted with different colors to facilitate their visualisation. This particular arrangement

can be generalized to any size of matrices with an even value of N, for $N \geq 6$, as follows:

1) in layer 1, all units are hybrid couplers, with coupling factors equal to 0.25π;
2) in layer 2, all units are crossover junctions, with coupling factors equal to 0.5π;
3) in layer n, for $n = 3 \ldots \frac{N}{2}$, the $\frac{N}{2} - n + 1$ units located at the center of the layer are crossover junctions;
4) in layer $\frac{N}{2} + 1$, no crossover junctions are used;
5) in layer n, for $n = \frac{N}{2} + 2 \ldots N - 1$, the $n - \frac{N}{2} - 1$ units located at the center of the layer are crossover junctions; and
6) all couplers in layer N are crossover junctions.

In standard Nolen matrices, the number of layers increases by two every time the number of beams increases by one, with a number of layers that may be expressed as $2N - 3$, for $N \geq 2$. Using Nolen matrices of size $N/2$, the corresponding number of layers is $N - 3$, to which 2 complete layers of crossover junctions have to be added before and after the standard matrices as well as a layer of hybrid couplers as first layer, thus demonstrating that the proposed matrix has exactly N layers.

As the proposed matrices rely on the combination of two Nolen matrices, the use of a parallel layout as described in [26] (see Fig. 2) is expected to provide a similar broadband response. Further investigations are required to define a systematic design procedure. It is anticipated that some assignments of phase differences p_n, for $n = 1 \ldots N$, may lead to simpler designs in terms of phase shifters and coupling factor imbalance required. The concept may also be extended to matrices with an odd number of beams. The Section III.E details the merits of the proposed matrices when compared to standard Nolen and Butler matrices.

E. COMPARISON WITH NOLEN AND BUTLER MATRICES

To complete this discussion on numerical examples, Table VI summarizes the minimum number of layers achieved with the proposed numerical method for matrices having two to eight beams where the values of θ and ϕ in all the units can be determined. For comparison, the number of layers in parallel Nolen matrices are also given. It is found that the minimum number of layers with the proposed matrix topology is smaller than that of Nolen matrices when the number of beams is larger than three. The benefits of this reduction in the number of layers were evidenced with the full-wave model described in Section III.B as the 5×5 parallel matrix occupies the same area as a 4×4 parallel Nolen matrix, both having 5 layers. The numerical results reported in this paper demonstrate that a number of layers equal to N is achievable for all the matrices analyzed, indicating this may be achieved for any size of matrix following the proposed design method. In fact, the proposed general form when N is even requires exactly N layers, and a similar general form may be found for odd values of N. Thus, the reduction in the number of layers, which may be expressed as $N/(2N - 3)$, will converge towards 50% as N becomes larger, which is a significant improvement. This reduction in the number of layers will naturally result in shorter overall transmission line lengths, leading to lower insertion losses. This is also expected to benefit the amplitude and phase dispersion over the operating bandwidth through the equalized path lengths and reduced number of components per electrical path from one input port towards any output port.

Another point of interest is the comparison of the proposed matrix with the well-known Butler matrix for number of beams equal to powers of two. While the matrix with four beams reduces to the standard Butler matrix, the matrix with eight beams is found to require less layers than the well-known configuration of Butler matrices defined with the conventional method relating to fast Fourier transform [10], requiring 10 layers [35] as illustrated in Fig. 8. The alternative layout reported in [36] also requires 10 layers. Interestingly, the standard Butler matrix requires only 12 couplers, while the proposed structure implements 16 couplers, confirming the topology equivalent to the fast Fourier transform is the one leading to the least number of components, although there is no known mathematical proof of it. Counting the crossover junctions, the standard 8×8 Butler requires 28 units, the same total of units as the proposed generalized matrix. However, our proposed arrangement leads to a reduced number of layers. The numerical design can be adapted for matrices with a number of beams larger than eight straightforwardly. It is anticipated that further reduction is achievable for larger matrices with a number of beams equal to a power of two, extending the particular topology illustrated in Fig. 8 and described in Section III.D. Other benefits of this newly proposed topology may become apparent as investigations progress on this topic.

IV. CONCLUSION

A novel family of generalized one-dimensional parallel switching matrices with an arbitrary number of beams has been presented. The minimum number of layers to determine the values of the parameters of the units for the matrices having two to eight beams has been provided as an illustration of the design method. A general topology for even values of beams was introduced, which requires exactly N layers, less than the $2N - 3$ layers of a standard Nolen matrix. As the value of N increases, the achieved reduction in the number of layers approaches a factor of two, which is significant and can result in more compact implementations. It was also found that the proposed matrix with eight beams requires less layers than well-known configurations of Butler matrices in planar implementation. Here as well, the reduction is expected to become more significant as the size of the matrix increases. The values of the parameters of the units for the matrices with four, five and eight beams have been given as numerical examples to illustrate the design method and confirm the potential of the proposed approach. A matrix formulation of the problem is also detailed, based on a layer matrix representation, enabling a parametric definition of the problem, suitable for numerical optimisation. The concept was further validated with a specific full-wave model of the 5×5 parallel matrix, confirming the anticipated benefits.

$$\mathbf{T}_1 = \begin{bmatrix} \cos\theta_1 e^{-j\phi_1} & -j\sin\theta_1 e^{-j\phi_1} & 0 & 0 \\ -j\sin\theta_1 & \cos\theta_1 & 0 & 0 \\ 0 & 0 & \cos\theta_2 e^{-j\phi_2} & -j\sin\theta_2 e^{-j\phi_2} \\ 0 & 0 & -j\sin\theta_2 & \cos\theta_2 \end{bmatrix}_{4\times 4} \tag{8}$$

$$\mathbf{T}_{2q+1} = \begin{bmatrix} \cos\theta_1 e^{-j\phi_1} & -j\sin\theta_1 e^{-j\phi_1} & 0 & \dots & 0 & 0 \\ -j\sin\theta_1 & \cos\theta_1 & 0 & \dots & 0 & 0 \\ 0 & 0 & \cos\theta_2 e^{-j\phi_2} & \dots & 0 & 0 \\ \vdots & \vdots & \vdots & \ddots & \vdots & \vdots \\ 0 & 0 & 0 & \dots & \cos\theta_{\frac{N}{2}} e^{-j\phi_{\frac{N}{2}}} & -j\sin\theta_{\frac{N}{2}} e^{-j\phi_{\frac{N}{2}}} \\ 0 & 0 & 0 & \dots & -j\sin\theta_{\frac{N}{2}} & \cos\theta_{\frac{N}{2}} \end{bmatrix}_{N\times N} \tag{9}$$

The method described is generic and can be advantageously applied to any size of matrix, overcoming the well-known limitation of standard Butler matrices. Thus, the proposed solution can be seen as an extension of the Butler matrix to any number of beams, and is considered a promising solution for the design of low-cost single-layer beam-switching matrices, particularly in the millimetre-wave range. The parallel implementation, resulting in equalized path lengths, combined with the reduction in the number of layers is expected to benefit the RF response of the matrix. This will be investigated further through specific designs in printed and waveguide technologies.

APPENDIX A
MATRICES WITH AN EVEN NUMBER OF BEAMS

Using the schematic representation in Fig. 3(a) and equation (2), the transmission matrix $\mathbf{T}_1$ of the first layer in a 4×4 matrix may be written as (8), shown at the top of the page.

This enables to identify the general form of the transmission matrix $\mathbf{T}_l$, for $l = 2q + 1$, q being an integer, corresponding to odd layers when N is even, which may be written as (9), shown at the top of the page.

Note that the indexes of the coupling factors and phase delays are relative to the layer in the general notations and do not correspond to the numbers reported in the schematic representations in this paper, except obviously for the first layer.

Similarly, the transmission matrix $\mathbf{T}_2$ of the second layer of the 4×4 matrix in Fig. 3(a) may be written as follows:

$$\mathbf{T}_2 = \begin{bmatrix} 1 & 0 & 0 & 0 \\ 0 & \cos\theta_3 e^{-j\phi_3} & -j\sin\theta_3 e^{-j\phi_3} & 0 \\ 0 & -j\sin\theta_3 & \cos\theta_3 & 0 \\ 0 & 0 & 0 & 1 \end{bmatrix}_{4\times 4} \tag{10}$$

This enables also to identify the general form of the transmission matrix $\mathbf{T}_l$, for $l = 2q$, q being an integer, corresponding to even layers when N is even, which may be written as (11), shown at the bottom of the page.

Cascading alternating odd and even transmission layers, one can produce a parametric representation of the complete transmission matrix $\mathbf{T}_{N\times N}$ of the proposed generalized matrix when N is even.

APPENDIX B
MATRICES WITH AN ODD NUMBER OF BEAMS

Using now the schematic representation in Fig. 3(b) and equation (2), the transmission matrix $\mathbf{T}_1$ of the first layer in a 5×5 matrix may be written as (12), shown at the top of the next page.

This enables to identify the general form of the transmission matrix $\mathbf{T}_l$, for $l = 2q + 1$, q being an integer, corresponding to odd layers when N is odd, which may be written as (13), shown at the top of the next page.

$$\mathbf{T}_{2q} = \begin{bmatrix} 1 & 0 & 0 & \dots & 0 & 0 & 0 \\ 0 & \cos\theta_1 e^{-j\phi_1} & -j\sin\theta_1 e^{-j\phi_1} & \dots & 0 & 0 & 0 \\ 0 & -j\sin\theta_1 & \cos\theta_1 & \dots & 0 & 0 & 0 \\ \vdots & \vdots & \vdots & \ddots & \vdots & \vdots & \vdots \\ 0 & 0 & 0 & \dots & \cos\theta_{\frac{N-2}{2}} e^{-j\phi_{\frac{N-2}{2}}} & -j\sin\theta_{\frac{N-2}{2}} e^{-j\phi_{\frac{N-2}{2}}} & 0 \\ 0 & 0 & 0 & \dots & -j\sin\theta_{\frac{N-2}{2}} & \cos\theta_{\frac{N-2}{2}} & 0 \\ 0 & 0 & 0 & \dots & 0 & 0 & 1 \end{bmatrix}_{N\times N} \tag{11}$$

$$\mathbf{T}_1 = \begin{bmatrix} \cos\theta_1 e^{-j\phi_1} & -j\sin\theta_1 e^{-j\phi_1} & 0 & 0 & 0 \\ -j\sin\theta_1 & \cos\theta_1 & 0 & 0 & 0 \\ 0 & 0 & \cos\theta_2 e^{-j\phi_2} & -j\sin\theta_2 e^{-j\phi_2} & 0 \\ 0 & 0 & -j\sin\theta_2 & \cos\theta_2 & 0 \\ 0 & 0 & 0 & 0 & 1 \end{bmatrix}_{5\times 5} \tag{12}$$

$$\mathbf{T}_{2q+1} = \begin{bmatrix} \cos\theta_1 e^{-j\phi_1} & -j\sin\theta_1 e^{-j\phi_1} & \dots & 0 & 0 & 0 \\ -j\sin\theta_1 & \cos\theta_1 & \dots & 0 & 0 & 0 \\ \vdots & \vdots & \ddots & \vdots & \vdots & \vdots \\ 0 & 0 & \dots & \cos\theta_{\frac{N-1}{2}} e^{-j\phi_{\frac{N-1}{2}}} & -j\sin\theta_{\frac{N-1}{2}} e^{-j\phi_{\frac{N-1}{2}}} & 0 \\ 0 & 0 & \dots & -j\sin\theta_{\frac{N-1}{2}} & \cos\theta_{\frac{N-1}{2}} & 0 \\ 0 & 0 & \dots & 0 & 0 & 1 \end{bmatrix}_{N\times N} \tag{13}$$

$$\mathbf{T}_2 = \begin{bmatrix} 1 & 0 & 0 & 0 & 0 \\ 0 & \cos\theta_3 e^{-j\phi_3} & -j\sin\theta_3 e^{-j\phi_3} & 0 & 0 \\ 0 & -j\sin\theta_3 & \cos\theta_3 & 0 & 0 \\ 0 & 0 & 0 & \cos\theta_4 e^{-j\phi_4} & -j\sin\theta_4 e^{-j\phi_4} \\ 0 & 0 & 0 & -j\sin\theta_4 & \cos\theta_4 \end{bmatrix}_{5\times 5} \tag{14}$$

$$\mathbf{T}_{2q} = \begin{bmatrix} 1 & 0 & 0 & \dots & 0 & 0 \\ 0 & \cos\theta_1 e^{-j\phi_1} & -j\sin\theta_1 e^{-j\phi_1} & \dots & 0 & 0 \\ 0 & -j\sin\theta_1 & \cos\theta_1 & \dots & 0 & 0 \\ \vdots & \vdots & \vdots & \ddots & \vdots & \vdots \\ 0 & 0 & 0 & \dots & \cos\theta_{\frac{N-1}{2}} e^{-j\phi_{\frac{N-1}{2}}} & -j\sin\theta_{\frac{N-1}{2}} e^{-j\phi_{\frac{N-1}{2}}} \\ 0 & 0 & 0 & \dots & -j\sin\theta_{\frac{N-1}{2}} & \cos\theta_{\frac{N-1}{2}} \end{bmatrix}_{N\times N} \tag{15}$$

Similarly, the transmission matrix $\mathbf{T}_2$ of the second layer of the 5×5 matrix in Fig. 3(b) may be written as (14), shown at the top of the page.

This enables also to identify the general form of the transmission matrix $\mathbf{T}_l$, for $l = 2q$, q being an integer, corresponding to even layers when N is even, which may be written as (15), shown at the top of the page.

Cascading alternating odd and even transmission layers, one can produce a parametric representation of the complete transmission matrix $\mathbf{T}_{N\times N}$ of the proposed generalized matrix when N is odd.

REFERENCES

[1] J. Blass, "The multidimensional antenna: A new approach to stacked beams," in *IRE Int. Conv. Record*, Pt. 1, vol. 8, pp. 48–50, Mar. 1960.

[2] J. Butler and R. Lowe, "Beam forming matrix simplifies design of electronically scanned antenna," *Elect. Design*, vol. 9, no. 8, pp. 170–173, Apr. 1961.

[3] J. Nolen, "Synthesis of multiple beam networks for arbitrary illuminations," Ph.D. dissertation, Bendix Corp., Radio Div., Baltimore, MD, Apr. 1965.

[4] N. J. G. Fonseca, A. Ali, and H. Aubert, "Cancellation of beam squint with frequency in serial beamforming network-fed linear array antennas," *IEEE Antennas Propag. Mag.*, vol. 54, no. 1, pp. 32–39, Feb. 2012.

[5] J. L. Allen, "A theoretical limitation on the formation of lossless multiple beams in linear arrays," *IEEE Trans. Antennas Propag.*, vol. 9, no. 7, pp. 350–352, Jul. 1961.

[6] W. K. Kahn and H. Kurss, "The uniqueness of the lossless feed network for a multibeam array," *IRE Trans. Antennas Propag.*, Vol. AP-10, pp. 100–101, Jan. 1962.

[7] N. J. G. Fonseca, "Discussion on reciprocity, unitary matrix, and lossless multiple beam forming networks," *Int. J. Antennas Propag.*, vol. 2015, pp. 1–9, Apr. 2015.

[8] K. Wu, M. Bozzi and N. J. G. Fonseca, "Substrate integrated transmission lines: Review and applications," *IEEE J. Microwaves*, vol. 1, no. 1, pp. 345–363, Jan. 2021.

[9] Y. J. Guo, M. Ansari and N. J. G. Fonseca, "Circuit type multiple beamforming networks for antenna arrays in 5G and 6G terrestrial and non-terrestrial networks," *IEEE J. Microwaves*, vol. 1, no. 3, pp. 704–722 Jul. 2021.

[10] J. P. Shelton and K. S. Kelleher, "Multiple beams from linear arrays," *IRE Trans. Antennas Propag.*, vol. 9, pp. 154–161, Mar. 1961.

[11] H. Hayashi, D. A. Hitko, and C. G. Sodini, "Four-element planar butler matrix using half-wavelength open stubs," *IEEE Microw. Wireless Compon. Lett.*, vol. 12, no. 3, pp. 73–75, Mar. 2002.
[12] C. Dall' *et al.*, "Design and realization of a 4 × 4 microstrip butler matrix without any crossing in millimeter waves,"*Microw. Opt. Technol. Lett.*, vol. 38, no. 6, pp. 462–465, 2003.
[13] M. Nedil, T. A. Denidni, and L. Talbi, "Novel Butler matrix using CPW multilayer technology," *IEEE Trans. Microw. Theory Techn.*, vol. 54, no. 1, pp. 499–507, Jan. 2006.
[14] Y. Ding and K. Wu, "A 4 × 4 ridge substrate integrated waveguide (RSIW) slot array antenna," *IEEE Antennas Wireless Propag. Lett.*, vol. 8, pp. 561–564, Apr. 2009.
[15] A. A. M. Ali, N. J. G. Fonseca, F. Coccetti, and H. Aubert, "Design and implementation of two-layer compact wideband Butler matrices in SIW technology for Ku-band applications," *IEEE Trans. Antennas Propag.*, vol. 59, no. 2, pp. 503–512, Feb. 2010.
[16] K. Wincza, S. Gruszczynski, and K. Sachse, "Broadband planar fully integrated 8 × 8 Butler matrix using coupled-line directional couplers," *IEEE Trans. Microw. Theory Techn.*, vol. 59, no. 10, pp. 2441–2446, Sep. 2011.
[17] T. Djerafi, N. J. G. Fonseca and K. Wu, "Design and implementation of a planar 4 × 4 Butler matrix in SIW technology for wideband applications," in *Proc. 40th Eur. Microw. Conf.*, Paris, France, Sep. 2010, pp. 910–913.
[18] T. Djerafi, N. J. G. Fonseca, and K. Wu, "Design and implementation of a planar 4 × 4 Butler matrix in SIW technology for wide band high power applications," *PIER B*, vol. 35, pp. 29–51, 2011.
[19] T. Djerafi and K. Wu, "A low-cost wideband 77-GHz planar Butler matrix in SIW technology," *IEEE Trans. Antennas Propag.*, vol. 60, no. 10, pp. 4949–4954, Oct. 2012.
[20] L.-H. Zhong, Y. Ban, J. Lian, Q. Yang, J. Guo, and Z. Yu, "Miniaturized SIW multibeam antenna array fed by dual-layer 8 × 8 Butler matrix," *IEEE Antennas Wireless Propag. Lett.*, vol. 16, pp. 3018–3021, Oct. 2017.
[21] I. Afifi and A.-R. Sebak, "Wideband 4 × 4 Butler matrix in the printed ridge gap waveguide technology for millimeter wave applications," *IEEE Trans. Antennas Propag.*, vol. 68, no. 11, pp. 7670–7675, Nov. 2020.
[22] E. T. Der, T. R. Jones, and M. Daneshmand, "Miniaturized 4 × 4 Butler matrix and tunable phase shifter using ridged half-mode substrate integrated waveguide," *IEEE Trans. Microw. Theory Techn.*, vol. 68, no. 8, pp. 3379–3388, Aug. 2020.
[23] N. J. G. Fonseca, "Printed S-band 4 × 4 Nolen matrix for multiple beam antenna applications," *IEEE Trans. Antennas Propag.*, vol. 57, no. 6, pp. 1673–1678, Jun. 2009.
[24] T. Djerafi, N. J. G. Fonseca, and K. Wu, "Planar Ku-band 4 × 4 Nolen matrix in SIW technology," *IEEE Trans. Microw. Theory Techn.*, vol. 58, no. 2, pp. 259–266, Jan. 2010.
[25] N. J. G. Fonseca and N. Ferrando, "Nolen matrix with tapered amplitude law for linear arrays with reduced side lobe level," in *Proc. 4th Eur. Conf. Antennas Propag.*, Barcelona, Spain, 2010, pp. 1–5.
[26] T. Djerafi, N. J. G. Fonseca, and K. Wu, "Broadband substrate integrated waveguide 4 × 4 Nolen matrix based on coupler delay compensation," *IEEE Trans. Microw. Theory Techn.*, vol. 59, no. 7, pp. 1740–1745, Jul. 2011.
[27] H. Ren, H. Zhang, and B. Arigong, "Ultra-compact 3 × 3 Nolen matrix beamforming network," *IET Microw. Antennas Propag.*, vol. 14, no. 3, pp. 143–148, 2020.
[28] P. Li, H. Ren, and B. Arigong, "A symmetric beam-phased array fed by a Nolen matrix using 180° couplers," *IEEE Microw. Wireless Compon. Lett.*, vol. 30, no. 4, pp. 387–390, Apr. 2020.
[29] H. Ren, H. Zhang, Y. Jin, Y. Gu, and B. Arigong, "A novel 2D 3 × 3 Nolen matrix for 2D beamforming applications," *IEEE Trans. Microw. Theory Techn.*, vol. 67, no. 11, pp. 4622–4631, Nov. 2019.
[30] J. P. Shelton, "Fast Fourier transforms and Butler matrices," *Proc. IEEE*, vol. 56, no. 3, pp. 350–350, Mar. 1968.
[31] W. Nester, "The fast Fourier transform and the Butler matrix," *IEEE Trans. Antennas Propag.*, vol. 16, no. 3, pp. 360–360, May 1968.
[32] S. P. Skobelev, "Methods of constructing optimum phased-array antennas for limited field of view," *IEEE Antennas Propag. Mag.*, vol. 40, no. 2, pp. 39–50, Apr. 1998.
[33] H. E. A. Laue and W. P. du Plessis, "A checkered network for implementing arbitrary overlapped feed networks," *IEEE Trans. Microw. Theory Tech.*, vol. 67, no. 11, pp. 4632–4640, Nov. 2019.
[34] N. Ferrando and N. J. G. Fonseca, "Investigations on the efficiency of array fed coherently radiating periodic structure beam forming networks," *IEEE Trans. Antennas Propag.*, vol. 59, no. 2, pp. 493–502, Feb. 2011.
[35] H. Moody, "The systematic design of the Butler matrix," *IEEE Trans. Antennas Propag.*, vol. 12, no. 6, pp. 786–788, Nov. 1964.
[36] T. N. Kaifas and J. N. Sahalos, "On the design of a single-layer wideband Butler matrix for switched-beam UMTS system applications [Wireless Corner]," *IEEE Antennas Propag. Mag.*, vol. 48, no. 6, pp. 193–204, Dec. 2006.

JIRO HIROKAWA (Fellow, IEEE) was born in Tokyo, Japan, in 1965. He received the B.S., M.S., and D.E. degrees in electrical and electronic engineering from Tokyo Institute of Technology (Tokyo Tech), Tokyo, Japan, in 1988, 1990, and 1994, respectively. From 1990 to 1996, he was a Research Associate and from 1996 to 2015, an Associate Professor with Tokyo Tech, where he is currently a Professor. From 1994 to 1995, he was with the Antenna Group, Chalmers University of Technology, Gothenburg, Sweden, as a Postdoctoral Fellow. He has authored or coauthored more than 200 peer-reviewed journal papers and more than 600 international conference presentations. His current research interests include analyses, designs, and fabrication techniques of slotted waveguide array antennas, millimeter-wave, and Terahertz antennas, and beam-switching circuits. During 1999–2003 and 2004–2007, he was an Associate Editor for the *IEICE Transactions on Communications*. From 2013 to 2016, he was also an Associate Editor and since 2016, has been the Track Editor of IEEE TRANSACTIONS ON ANTENNAS AND PROPAGATIONS. He was the Chair of the Technical Program Committee for ISAP 2016. From 2017 to 2019, he was also the Chair of the IEICE Technical Committee on Antennas and Propagation. He was the recipient of the IEEE AP-S Tokyo Chapter Young Engineer Award in 1991, the Young Engineer Award from IEICE in 1996, the Tokyo Tech Award for Challenging Research in 2003, the Young Scientists' Prize from the Minister of Education, Cultures, Sports, Science and Technology in Japan in 2005, the Best Paper Award in 2007 and the Best Letter Award in 2009 from IEICE Communications Society, and the IEICE Best Paper Award in 2016 and 2018. He is a Fellow of IEICE.

NELSON J. G. FONSECA (Senior Member, IEEE) received the M.Eng. degree in electrical engineering from the Ecole Nationale Supérieure d'Electrotechnique, Electronique, Informatique, Hydraulique et Télécommunications, Toulouse, France, in 2003, the M.Sc. degree in electrical engineering from the Ecole Polytechnique de Montreal, Montreal, QC, Canada, in 2003, and the Ph.D. degree in electrical engineering from Institut National Polytechnique de Toulouse - Université de Toulouse, Toulouse, France, in 2010.

He is currently an Antenna Engineer with the Antenna and Sub-Millimetre Waves Section, European Space Agency (ESA), Noordwijk, The Netherlands. Since November 2020, he has been an Honorary Professional Fellow with the University of Technology Sydney, Sydney, NSW, Australia. He has authored or coauthored more than 230 papers in peer-reviewed journals and conferences and has more than 50 patents issued or pending. His research interests include multiple beam antennas for space missions, beamformer theory and design, ground terminal antennas, transfer of technology from and to terrestrial systems, including 5G networks, and novel manufacturing techniques.

Dr. Fonseca was the Chair of the 38th ESA Antenna workshop in 2017, and the Co-Chair of the 2018 IET Loughborough Antennas & Propagation Conference. He is currently an Associate Editor for the *IET Microwaves, Antennas and Propagation* and for IEEE TRANSACTIONS ON MICROWAVE THEORY AND TECHNIQUES, and a Topic Editor of IEEE JOURNAL OF MICROWAVES. He is also the Co-Vice Chair of the newly founded IEEE MTT-S Technical Committee 29 on Microwave Aerospace Systems. Since January 2019, he has been a Board Member of the European School of Antennas and Propagation (ESoA) and is also the coordinator of the ESA/ESoA course on Antennas for Space Applications, for which he was voted best Lecturer by the participants of the 2020 edition. He is the elected EurAAP Regional Delegate representing Benelux for the term 2021–2023. He was the recipient of various prizes and awards, including the Best Young Engineer Paper Award at the 29th ESA Antenna Workshop in 2007, the ESA Teamwork Excellence Award in 2020, and multiple ESA technical improvement awards.